ANALYSIS OF THE FLUID DYNAMIC BEHAVIOR OF THE REVERSE OSMOSIS DESALINATION PROCESS FOR DIFFERENT GEOMETRIES OF SPACERS

Gilsomaro Barbosa de Melo Silva[1], Francisco Samuel Chaves[1], Diego David Silva Diniz[1], Jackson de Brito Simões [1]

[1]Departament of Science and Technologya, Rural Federal University of the Semi-Arid
RN-233, Zip Code 59780-000, Caraúbas-RN, Brazil.
gilsomaro.silva@alunos.ufersa.edu.br, samuel_tab_1996@hotmail.com, diego.diniz@ufersa.edu.br, jackson.simoes@ufersa.edu.br

Abstract. Water scarcity is a problem that has affected humanity for decades and, in recent years, has been getting worse, even more so with global warming, population growth, and droughts. Therefore, desalination processes have been seen as essential alternatives for producing drinking water around the world. Finally, several technologies are used for the desalination of brackish water; among these techniques, desalination by membrane separation processes via reverse osmosis (RO) stands out, a promising technology, considering that it is a simple process and presents low investment. However, the disadvantage that there is in its use is the sensitivity of the membrane to fouling. In this context, this work aimed to define computational modeling capable of understanding the behavior of the reverse osmosis process from different spacer geometries. The mathematical model used to carry out the simulations was based on mass conservation equations, movement, species transport, and Spiegler and Kedem's model. All simulations were performed using the ANSYS FLUENT software and ICEM CFD to create the geometry and the mesh. The simulation results showed a good representation of the transfer phenomena involved in the reverse osmosis separation process; moreover, these results enabled a detailed analysis of fluid behavior under the effects of turbulence promoters in the flow channel to be permeated. Finally, when analyzing these parameters, it was observed that the lozenge-type spacers had better process performances in the geometries studied.

Keywords: Computational modeling, Desalination, Turbulence promoters.

1 Introduction

The scarcity of water is a problem that has affected humanity for decades and, in recent years, has been getting worse with global warming, population growth, and record droughts, so that desalination processes began to be seen as essential alternatives for the production of drinking water, with the mastery of technologies of desalination, incredibly reverse osmosis, the potential exploitation of groundwater for the human consumption. The desalination process removes excess mineral salts, impurities, and other microorganisms found in brackish water to obtain drinking water [1] [2].

Reverse osmosis is an operation in which the solvent is separated from the solution by passing it through a semipermeable membrane developed to retain salts and solutes with low molecular weights. In the osmosis process, the solvent flows through the membrane from a solution of low concentration to a more concentrated one until the elevation of static pressure ("osmotic pressure") on the side of the concentrate prevents flow. In Reverse Osmosis (R_O), the direction of water flow is reversed when, in the process and over the more concentrated solution, a pressure more significant than the osmotic pressure is applied. This way, water of low saline concentration water moves into a saline solution. However, the downside that there is in the use of this process of desalination by reverse osmosis is related to the useful life of the membranes semipermeable in the equipment; this disadvantage entails, throughout the process, low permeate flow rate and or high passage of solute, thus affecting the productivity of the system and consequently reducing the useful life of the equipment [2].

To minimize these adverse effects and increase the permeate flux, spacers promote turbulence in the feed stream and decrease the concentration layer on the membrane. In addition to increasing the permeable flow, these spacers also facilitate an increase in the pressure drop and, consequently, in the energy used.

Because of the above, the main objective of this work is to build computational modeling capable of predicting the desalination process via R_O, employing the equations of conservation of mass, linear momentum, and species transport and, thus, analyze the influence of different geometries of these spacers in the process of desalination by R_O.

2 Theoretical reference

2.1 Desalination

The desalination process treats brackish water, promoting the removal of dissolved minerals. Among the various current desalination techniques, the one that has stood out the most industrially is the membrane separation process, as it has superiority in producing water capacity. The separation processes by membranes have shown rapid growth due to their requirements for high energy efficiency, easy maintenance, lower area occupation, quick initiation, and good cost-effectiveness, influencing cost reduction and global desalination rates over the last decade [3].

However, there are some limitations during this process, and these are linked to concentration polarization and scale formation, which lead to reduced permeate flow, increased operating pressure, inadequate selectivity, shorter membrane duration, and increased operating costs, also decreasing the useful life of the equipment [4].

About membrane technologies, [5] refer to the following methods: Electrodialysis and Reverse Osmosis; however, this work will stop at the process of RO.

2.2 Osmosis and Reverse Osmosis

Osmosis is a naturally occurring physical-chemical phenomenon when a semipermeable membrane separates two liquids with different levels of concentration of salt in solution. During this process, the solvent from the more dilute liquid naturally diffuses through the membrane towards the more concentrated one. The process continues until it reaches a point of equilibrium when the solution levels balance out [6]. Reverse osmosis, in turn, is the reversal of this natural flow. The water from the salt solution is forced across the membrane in the opposite direction by applying an external pressure above the osmotic pressure. When a pressure higher than the osmotic pressure is applied to the saltier side of the membrane, the water flow is reversed and begins to flow from the salty side to the pure side of the membrane solution [7].

Figure 1 is a schematic representation of the reverse osmosis process, in which a pump is applied in one of the process channels, the channel and feed, to obtain a pressure more significant than the osmotic and thus forces the flow of water in the membrane.

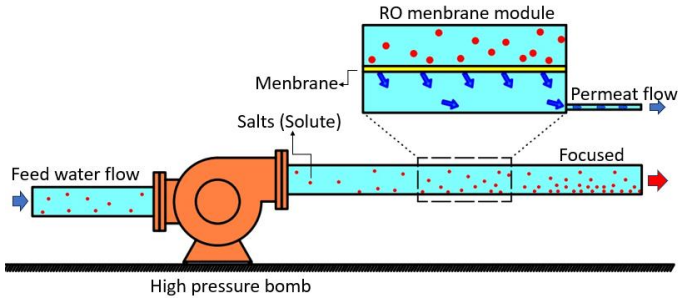

Figura 1. Esquema de um processo de osmose reversa.

This type of desalination system via reverse osmosis is considered to be more energy efficient when compared to other kinds of processes [8], and its main disadvantage is the use of membrane sensitivity for scales.

2.3 Reverse Osmosis Equipment

There are many devices designed to carry out R_O, including microfiltration (MF), ultrafiltration (UF), nanofiltration (NF), and R_O [6]. The main constituent elements of this equipment are the high-pressure pump, permeation module, semipermeable membranes, and turbulence promoters. The two latter being the most important in the process, including the possibility of changing characteristics to improve the procedure.

The membranes are versatile components. Their primary objective is to allow the passage of liquids and, simultaneously, prevent salts from being transported. Makes as these residues of salts taken from the water are present in the regions where the membrane is located. To minimize the unfavorable effects, spacers are used to promote turbulence in the feed flow and decrease the layer of salt concentration in the membrane [9].

These spacers are elements that make up the spiral module that directly affect the performance of the membrane. In addition, this type of component encourages an increase in mass transport, reducing the solution concentration. On the wall and fouling [4]. Figure 2 highlights in a simplified way the main components present

in a spiral-type permeation module. The desalination process occurs according to arrows indicating the directions and direction of flow within a permeation module.

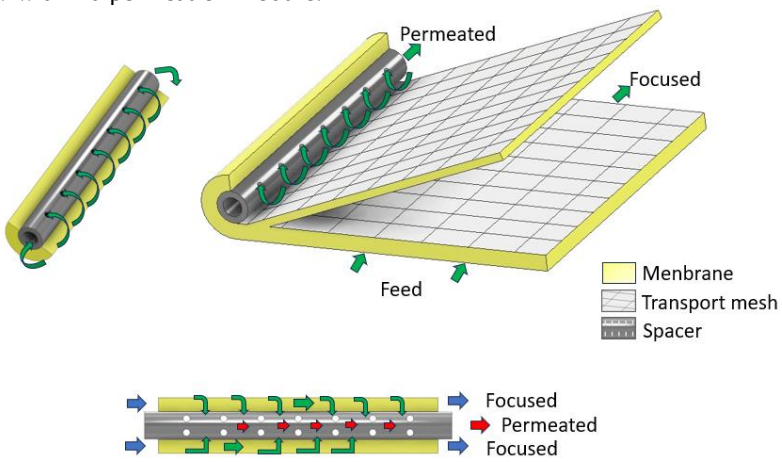

Figura 2. Elemento de membrana em espiral para o processo de osmose reversa.

Using spacers as turbulence promoters allows the creation of turbulent flow that, in addition to increasing permeable flow, can also help reduce polarized boundary layers and fouling problems.

3 Methodology

The research of this work is linked to the modeling and simulation of a study domain that can represent the physical phenomena that occur in a permeation module with a reverse osmosis membrane.

The software used was ANSYS ICEM CFD for constructing the domains and their meshes and ANSYS FLUENT for the numerical solution of the models and analysis of results.

3.1 The geometry of the feed channel domains

The geometries to characterize the region and zones of interest were built in the ANSYS ICEM CFD software. Thus, a geometry with an empty channel (without a spacer) and another one with a channel for each spacer geometry with a submerged type arrangement was modeled to carry out the simulations.

The geometries with and without spacers were built with main dimensions: 69 x 2 mm (length x height of the feed channel). Five geometric shapes for the spacers were investigated. Figure 3 shows the geometry without a spacer that was used to compare the results in the fluid dynamic analysis. All proposed constructions were carried out based on dimensionless relationships between channel size values and their spacer dimensions. These relationships can be found in the works of [11] [12].

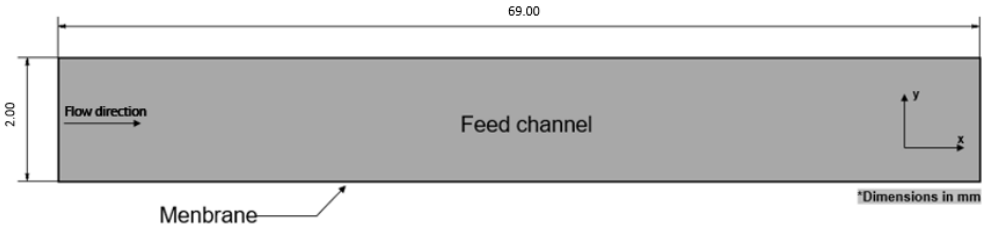

Figure 3. Channel geometry without spacer.

Based on the work of [4] and the relationships of the dimensions, the values of the distance between the beginning of the feed channel and the centroid of the first filament of 12 mm, the distance between the centroids of the 8 mm spacers and the distance between the centroid of the last filament and the end of the feed channel of 25 mm were constructed, as shown in Figure 4.

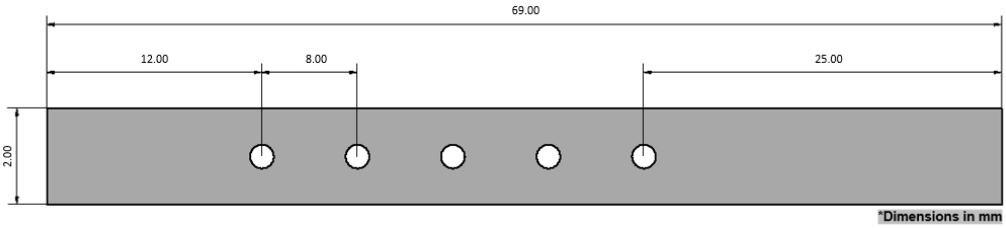

Figure 4. Channel geometry with circular spacers.

3.2 Geometry of spacer domains

The five different types of geometries for spacers used, having the shapes of circle, isosceles triangle, rhombus, square, and hexagon with their respective dimensions, are presented in Figure 5.

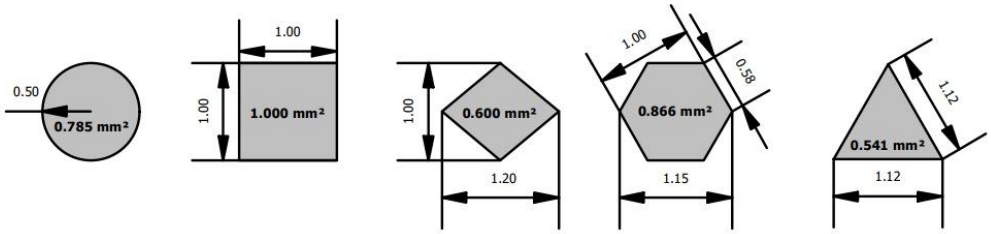

Figure 5. Geometries of the spacers under analysis (Dimensions in mm).

3.3 Generation of numerical meshes

The computational domain models were constructed using the ANSYS ICEM CFD software since when using finite volumes as a discretization method to solve equations, it is necessary to build a mesh numerical for each domain under study. After modeling the geometries, the fluid input and output zones, walls, and the interface with the membrane conditions were defined, then the blocking, the pre-mesh, and the conversion of the output element of the file mesh to ANSYS FLUENT.

For the construction of the meshes, an increase in the density of cell numbers close to both the membrane surface and the spacers was performed, due to the presence of factors that cause a more significant gradient in the variable constituents of the process, such as the polarization of the concentration. This fact is reported in the works of the authors [10]. The authors [12] recommend that the height of the first cell closest to the surfaces should be magnitudes less than $2{,}5x10^{-7}$ meters. Figure 6 highlights the mesh refinement regions at the locations near the area where the membrane effect was modeled.

In addition, the mesh was refined in the regions close to the spacers to ensure that the values found for the study were the most relative to the analytical values. Then, the quality of the meshes was evaluated using the quality criterion of the ICEM CFD, in which it was concluded that the meshes showed values above 0.8 and were considered satisfactory, as seen in [4].

Figure 6. Refinement of the mesh near the membrane area.

3.4 Modeling the physical properties of the solution and boundary conditions

The study consists of a solution that flows in the feeding channel and membrane, where this solution is composed of water and a sodium chloride (NaCl) solute. The physical properties of this solution vary as a function of the solute mass fraction (ma) at a temperature of 25.0 ± 0.5 ºC and using a parameter with the Reynolds number in the *inlet* of 70 for all domains. Thus, the authors [13] suggested equations representing the density (ρ), viscosity

(μ), and diffusivity (DAB) of the solution at a density for a mass fraction of (NaCl) less than 0.09 kg/kg. These values are presented in Table 1.

Table 1. Polynomial functions describe the values of density, viscosity, and diffusivity.

Property	Equations
Density (ρ)	$\rho = 997.1\ (1 + 0.696 m_a)$
Viscosity (μ)	$\mu = 0.89(1 + 1.63ma\ )10^{-3}$
Difusividade (D_{AB})	$D_{AB} = \begin{cases} 1.61(1 - 14m_a)10^{-9}, & ma < 0.006 \\ 1.45x10^{-9}, & , \ max < 0.006 \end{cases}$

The inlet boundary conditions are defined by the input of a fully developed flow with a mass fraction of sodium chloride of ma= 0.002 kg/kg. Such value was taken as the basis of the works of [4], [10]. The average inlet velocity (u) is indicated by the Reynolds number on the inlet front. For the outlet conditions, the pressure was applied to the outlet of the concentrate, which is greater than the atmospheric pressure applied at the permeate outlet. This output condition considers the flow fully developed. For the walls, it was considered a fact that there is no slip and that the walls are waterproof. For the geometries with spacers, surfaces were defined as impermeable and without slipping.

Finally, for the adopted modeling, the membrane was defined as a semipermeable wall without sliding and was based on the mathematical modeling presented by [12]. The equations used to describe the effects of the membranes were from the Spiegler and Kedem model and the film theory. Following [10], data were obtained experimentally for an aqueous solution of NaCl in an empty membrane channel, such as $\Delta p = 8.103 \times 10^5$ Pa and a fraction of the mass of 0.002 kg/kg. The values are of salt rejection R = 0.99 and the membrane resistance constant $Rm = 1.562 \times 10^{14}$ m^{-1}. Table 2 highlights in a simplified way the equation applied to the input, wall, membrane, and output conditions.

Table 2. Equation adapted for the conditions of the zones.

Zon	Boundary condition
Inlet	$u = 6\bar{u}\frac{y}{h}\left(1 - \frac{y}{h}\right), \quad v = 0, \quad m_a = m_a^{inlet}$
Wall	$u = 0, \quad v = 0, \quad \frac{\partial m_a}{\partial y} = 0$
Membrane	$u = 0, \quad v = J_w = \pm\frac{1}{R_m \mu}(\Delta p - \sigma\Delta\pi), \quad m_a = m_a^{sp}$
Outlet	$\frac{\partial u}{\partial x} = 0, \quad \frac{\partial v}{\partial x} = 0, \quad \frac{\partial m_a}{\partial x} = 0, \quad p_A = p_a^{outlet}, \quad p_B = p_{atm}$

For implementations of the equations in ANSYS FLUENT, it was necessary to include and develop computational routines in C language (UDFs). The numerical solution methods adopted in the proposed studies were: the Least Squares Cell-Based methods for gradient determination; for the discretization of the pressure and momentum equations, the second-order Upwind was used, and for the discretization of the species equations, the first-order Upwind method was used. And finally, the SIMPLE (Semi-Implicit Method for Pressure Linked Equations) algorithm was selected, which works in the phase related to the solution of the equations of motion and the equation of average, was chosen.

Regarding mathematical modeling, all the domains performed in this study were treated in a permanent regime, considering an isothermal and adiabatic process, and the effect of gravity was disregarded. In the simulations, the initial conditions in the solution were with initial velocity values adopted for the cells in the feeding zone and the mass fraction of NaCl with a value of zero and the chosen number iterations of 10000 and a convergence criterion of $1x10^{-7}$, where it had good results.

4 Results

The influence of spacer types on fluid dynamics and mass transfer in the RO process is presented in this work to verify the importance of spacers in the combat of the polarized layer. Thus, the simulations for a two-

dimensional domain with circular spacers arranged in a submerged arrangement, with a diameter of 1 mm, are presented in figures 7, 8, and 9, highlights in which it is possible to observe the influence of the presence of spacers influences the behavior of the flow and mass distribution.

In Figure 7, it is observed that the presence of spacers directs the flow of fluid to the membrane and the wall of the domain, resulting in a high-speed local field that increases the drag force of the solution in the vicinity of the membrane surface and, as a result, causes removal of part of the solute in the region, a local cleanup process taking place. However, due to the low pressure and the shape of the flow that forms immediately after the spacer, the flow tends to align in the middle of the channel, creating a "comet syrup," slowing it down and reducing the effect of drag near the membrane. This stimulates the formation of stagnation regions, accumulating the solution between the filaments in the following area, which increases the thickness of the polarized concentration layer. Such effects were also observed in the work of [4]. This phenomenon occurred for all geometries analyzed.

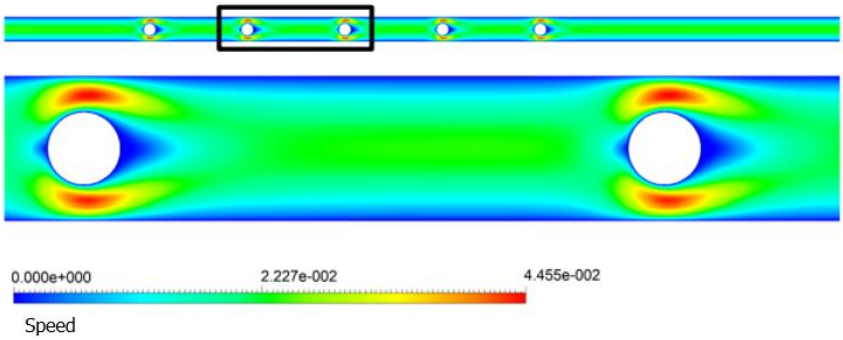

Figure 7. Velocity field in m/s for a domain with circular spacer.

Figure 8 highlights the influence of spacers on the polarized layer, in which there is a tendency of displacement of the solute towards the posterior spacer; as a consequence, there is a more significant increase in the thickness of the layer closest to the region of the other spacer. This is caused by the rise in the drag force motivated by the increase in velocity, which provides immense energy to detach the solute from the surface of the membrane or the region with lower velocity values. The phenomenon was also observed in the other geometries analyzed.

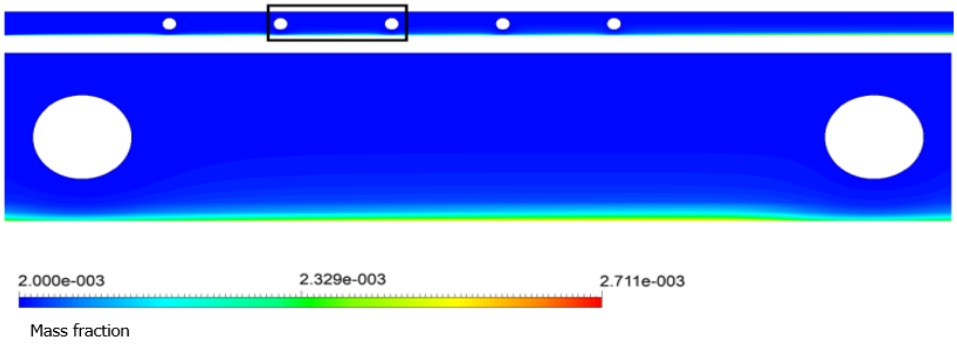

Figure 8. Mass fraction for a domain with circular spacer.

Figure 9 compares the domain's polarization concentration factor (Γ) with circular spacers and without spacers as a function of the dimensionless length along the membrane surface. By comparing the curves, it is possible to observe the spacers' effect, causing a change in the mass behavior of the flow. This causes a decrease in the polarization concentration factor, causing a reduction in the concentration of the solute in the membrane. Such behavior is observed by [12], and the results are similar to those obtained in the works of [4].

Based on the results obtained in Figure 9 using the metric of the mean of the polarization concentration factor for the cases with circular spacers, it was possible to quantify this effect, producing median values of 0.01065065 for the curve with spacer and 0.017757 for the curve without the use of spacers, obtaining a reduction of 40% in the importance of $\Gamma_{méd}$ along the surface. Regarding the pressure loss per unit length (P/L) caused by the presence of spacers, the value is 138.58 Pa/m, which corresponds to 3.38 times the value without the use of spacers.

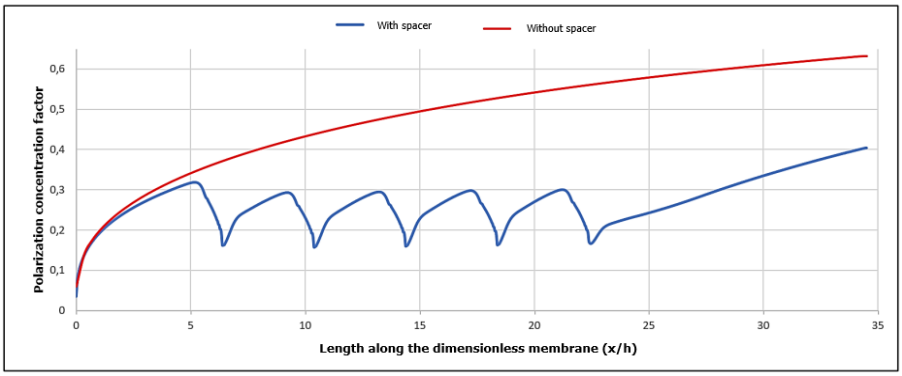

Figure 9. Curves of the factor Γ for a domain with circular spacer and without spacer.

The performance of different spacer configurations and geometries was analyzed, and Equation 1 was used to calculate the Spacer Performance Ratio (SPMP). The Spacer Performance Ratio (SPMP) was used, which is calculated using Equation 1. Such an equation was used to quantify the comparison between cases, according to [14]. Where ΔC represents the mass fraction concentration difference, and ΔP is the pressure difference between the outlet and inlet of the feed channel. A spacer is more efficient when it has the highest SPMP value among the analyzed promoters.

$$SPMP = \frac{\Delta \text{Cspacer} \,/\, \Delta \text{C without spacer}}{\Delta \text{Pespacer} \,/\, \Delta \text{P without spacer}} \qquad (1)$$

Based on the analyses presented, the same configuration and identical setups were used in the simulations in the other geometries of the isosceles triangle, diamond, square, and hexagon type, thus obtaining results that are represented in Table 3. Table 3 shows the values of the mass fraction difference, the pressure loss per unit length (P/L) found, and the SPMP calculated for each case.

Table 3. SPMP values for cases with submerged arrays.

Geometry	**Δc (10^{-3})**	**ΔP/L**	**SPMP**
Without spacer	6.38	41.03	-
Circle	2.44	138.58	0.1134103
Triangle	2.06	145.04	0.0914635
Square	1.65	217.43	0.0487999
Diamond	2.43	117.04	0.1334301
Hexagon	1.39	238.98	0.0343110

Figure 10 shows the mean values of the SPMP parameters for the different spacer geometries studied. The results obtained through the simulations agree with the results found by [14] in his work, where SPMP values increase for filaments with smaller diameters for any configuration. Because, compared to the empty channel, the pressure loss decreases significantly with the filament area. When comparing the data obtained by the SPMP parameters, it is possible to observe that the geometry of the lozenge-type spacer received the most satisfactory values.

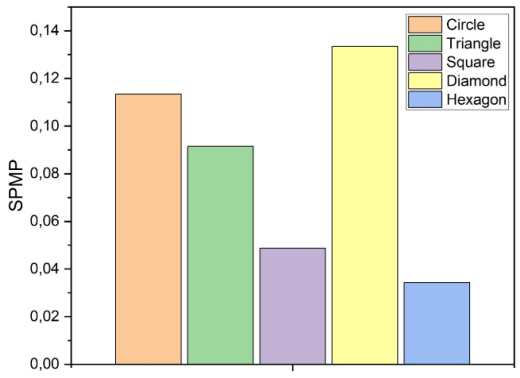

Figure 10. Mean SPMP values of the spacers studied.

5 Conclusion

The methodology and numerical modeling employed in this work proved to be adequate for the objective of the research, being possible to evaluate the hydrodynamic and mass behavior of the desalination process, being able to predict the formation of the polarization layer by concentration, phenomena typically present in the membrane desalination process.

By the general analysis of the results of this research, it was possible to observe that the spacers promote changes in the velocity fields and, consequently, in the distribution of the mass fraction of salts. The presence of spacers promotes an increase in local velocity in their vicinity, as there is a localized choke where turbulence promoters are present.

In addition, it can be noted that due to the low pressure, added to the formation of the mat right after the spacer and, thus, the flow tends to align itself in the middle of the channel, decreasing its speed near the membrane and, consequently, the drag effect on the deposited solute. Promotes an accumulation of solute in the subsequent region between the filaments, which causes an increase in the thickness of the polarized concentration layer.

Finally, based on the values obtained by the SPMP parameter, the geometries with the best results are those with the best balance between head loss and the production capacity of the final product. Therefore, the geometry with diamond spacers presented the best SPMP values among the geometries studied in this work.

References

[1] SILVA, Akleino Silvestre. Modelagem e simulação da dessalinização de águas salobras usando um separador ciclônico térmico munido de bicos aspersores akleino silvestre da silva. 2016. Universidade Federal de Campina Grande, [s. l.], 2016.

[2] SOUSA, Paula Cristina dos Santos. Estudo da hidrodinâmica em canais de alimentação de uma membrana de dessalinização. 2013. Universidade De Trás-Os-Montes E Alto Douro, [s. l.], 2013.

[3] Bahar, Rubina; Hawlader, Mohammad Nurul Alam, 2013. Desalination: Conversion of seawater to freshwater. 2nd International Conference on Mechanical, Automotive, and Aerospace Engineering - ICMAAE 2013, Brasil.

[4] Diniz, D. D. S., 2021. Estudo da fluidodinâmica da dessalinização das águas salobras via osmose reversa: modelagem e simulação. 2021. 248f. Tese de Doutorado, Programa de Pós-Graduação de Engenharia de Processos, Universidade Federal de Campina Grande, Campina Grande, Brasil.

[5] Younos, T.; Tuluo, K.E. *Overview of Desalination Techniques. Journal of Contemporary Water Research & Education Issue.* Universities Council on Water Resources, 3-10, 2005.

[6] Moura, J. P.; Monteiro, G. S.; Silva, J. N.; Pinto, F. A.; França, K. P. Aplicações Do Processo De Osmose Reversa Para O Aproveitamento De Água Salobra Do Semi-Árido Nordestino. Revista águas subterrâneas, [s. l.], 2008.

[7] Baker, R. W. Membrane Technology and Applications. Second Edition. John Wiley & Sons, 2004. ISBN: 0-470-85445-6.

[8] Miller, S.; Shemer, H.; Semiat, R. Energy and environmental issues in desalination. Desalination, v. 366, p. 2–8, 2015.

[9] Proença, M. P, 2009. Desenvolvimento de Membranas Íon-Seletivas com Poliestireno Sulfonado e Polianilina Dopada para a Aplicação em Eletrodiálise. Dissertação de Mestrado – Escola de Engenharia – Universidade Federal do Rio Grande do Sul, Porto Alegre.

[10] Amokrane, Mounir; Sadaoui, Djamel; Dudeck, Michel; Koutsou, Chrysafenia P, 2016. New spacer designs for improving the zigzag spacer configuration performance in spiral-wound membrane modules. Desalination and Water Treatment, Vol. 57, pág. 5266–5274, 2016.

[11] Keir, Gregory Peter. Coupled modeling of hydrodynamics and mass transfer in membrane filtration by. Separation and Purification Technology, [s. l.], n. Hons I, 2012.

[12] Ahmad, A. L. L.; Lau, K. K.; Bakar, M. Z. Z. Ab, 2005.; Shukor, S. R. Abd. Integrated CFD simulation of concentration polarization in narrow membrane channel. Computers e Chemical Engineering, Vol. 29, pág. 2087–2095.

[13] GERALDES, Vítor; SEMIÃO, Viriato; DE PINHO, Maria Norberta. Flow and mass transfer modeling of nanofiltration. Journal of Membrane Science, [s. l.], v. 191, n. 1– 2, p. 109–128, 2001.

[14] Schwinge, J.; Wiley, D. E.; Fletcher, D. F. Simulation of the flow around spacer filaments between channel walls. 2. Mass-transfer enhancement. Industrial and Engineering Chemistry Research, [s. l.], v. 41, n. 19, p. 4879–4888, 2002.